Penning Ionization of Cyclopropanes by Collision with He*(2^3S) Metastable Atoms

Hideo Yamakado,† Tetsuji Ogawa, and Koichi Ohno*

Department of Chemistry, Graduate School of Science, Tohoku University, Aramaki, Aoba-ku, Sendai 980-77, Japan

Received: January 17, 1997; In Final Form: March 26, 1997[⊗]

The Penning ionization of cyclopropane (C_3H_6), cyclopropylamine ($C_3H_5NH_2$), and cyanocyclopropane (C_3H_5-CN) upon collision with He*(2^3S) metastable atoms was studied by collision energy resolved Penning ionization electron spectroscopy. Collision energy dependence of the partial ionization cross sections indicated that the interaction potentials are strongly anisotropic between He*(2^3S) and the investigated cyclopropanes. In the studied energy range, the interaction potential was found to be attractive around the amino and cyano groups. A repulsive interaction potential was found around the carbon ring and hydrogen atoms for cyclopropane, and the order of the hardness was C_3 ring (out-of-plane direction) < hydrogen atoms < C_3 ring (in-plane direction). These are consistent with calculated interaction potential curves.

I. Introduction

Interaction potentials between molecules and atoms are important since they are strongly related to the mechanism of the chemical reactions. In a chemi-ionization process known as Penning ionization,[1−3] a molecule M collides with a metastable atom A* having an excitation energy much larger than the lowest ionization potential (IP) of the molecule. This process yields the ground-state atom A, one of the ionic states of the molecule M_i^+, and an ejected electron e^-:

$$A^* + M \rightarrow A + M_i^+ + e^- \quad (1)$$

The measurements for the intensity of the positive ions or electrons would give the total ionization cross section, σ_T. Collision energy (E_c) dependence of σ_T reflects the details of the interaction potential.[2,4]

Total ionization cross sections for various atoms and simple molecules have been extensively investigated in previous years.[4−11] For example, the attractive potential for Hg[2,4,8] atom and repulsive potential for Ar[4−8] atom have been found. For anisotropic molecules, it is difficult to obtain information on anisotropic interaction potentials because the collision energy dependence of $\sigma_T(E_c)$ reflects only an average potential.

In Penning ionization electron spectroscopy (PIES),[12] the kinetic energies of electrons ejected by Penning ionization are analyzed. Since a given ionic state of a closed-shell molecule is usually ascribed to the ionization of a molecular orbital, which is more or less localized on a special part of the molecule, collision energy dependences of partial ionization cross sections $\sigma(E_c)$ reflect information about the anisotropy of the interaction potential.

Recently, coupled techniques including velocity selection and electron energy analysis have been developed.[13−19] Velocity-controlled supersonic metastable beams have been utilized to measure the collision energy resolved PIES (CERPIES) of Ar by collision with He*(2^1S,2^3S).[17−19] In our recent papers,[13−16,20−27] using the time-of-flight (TOF) method, we reported the collision energy dependence of the partial ionization cross sections (CEDPICS) $\sigma(E_c)$ and information on the anisotropic interaction potentials for some molecules. In these studies, strong attractive interactions with He*(2^3S) were found for local regions around the oxygen atom of the C═O group of HCHO (formaldehyde) and CH_2CHCHO (acrolein).[22] For some nitriles,[23,26] a strong attractive interaction around the CN groups has been found, and for CH_3NC,[23] the interaction around the NC group has been found to be weaker. The interaction potential between He*(2^3S) and CH_3NCO, CH_3NCS, and CH_3-SCN has also been found to be attractive around the pseudohalide π orbitals and repulsive around the methyl group.[20] An especially strong attractive potential has been observed in the terminal nitrogen and oxygen "lone electron pair" regions of CH_3SCN and CH_3NCO.[20] For methanol and ethers, attractive potentials around the oxygen atom and repulsive potential around the alkyl group have been found.[24,27] For some saturated and unsaturated hydrocarbons, it has been indicated that the interaction potential is attractive near the π orbital region; otherwise, it is repulsive.[16]

Since a He*(2^3S) atom resembles a Li atom in its characteristics as described in section III, observed attractive interactions suggest the existence of a stable Li complex of these compounds. In recent experimental studies, such Li complexes have been reported.[28]

In this paper, we investigated the interaction potential between the He*(2^3S) atom and some cyclopropanes: cyclopropane, cyclopropylamine, and cyanocyclopropane. Interaction potentials around the carbon ring and the amino and cyano groups are discussed.

II. Experiment

The experimental apparatus used in this work has been reported in previous papers.[13−16] Metastable atoms of He*-(2^3S,2^1S) were produced by a discharge nozzle source, and the He*(2^1S) component was quenched by a water-cooled helium discharge lamp. The kinetic energies of electrons ejected by collisional ionization were determined by a hemispherical electrostatic deflection type analyzer[29] using an electron collection angle 90° to the incident He*(2^3S) beam axis. The energy resolution of the electron analyzer was estimated to be 40 meV from the full width at half-maximum (fwhm) of the $Ar^+(^2P_{3/2})$ peak in the He I ultraviolet photoelectron spectrum (UPS).

In the collision energy resolved measurements, the metastable beam of He*(2^3S) was chopped by a mechanical chopper with

† Present address: Department of Material Science and Chemistry, Faculty of System Engineering, Wakayama University, Sakaedani, Wakayama 640, Japan.

⊗ Abstract published in *Advance ACS Abstracts,* May 1, 1997.

S1089-5639(97)00259-4 CCC: $14.00

2 mm wide slits to produce a pulsed metastable beam, and the resolution of the electron energy analyzer was lowered to 250 meV (fwhm for He I UPS of Ar) in order to obtain higher counting rates of electrons. A TOF spectrum $I_M(t)$ of the pulsed He*(2^3S) beam with sample molecules in the collision cell was obtained by detecting emitted electrons from a stainless steel plate inserted at the center of the collision cell. The time-of-flight of secondary electrons from the metal surface to the detector is negligibly short in comparison with the TOF of the He* atoms. The efficiency of the secondary electron from a metal (stainless steel) plate was considered to be constant in the observed collision energy range.[14]

In order to measure CERPIES, two spectra with a low collision energy of about 100 meV and a high collision energy of about 250 meV were recorded for each molecule in the present study.

In the CEDPICS measurement mode, the time-dependent spectrum of Penning electrons for a given ionic state, $I_E(t)$, was measured using the energy fixed mode of the electron analyzer. Since the time-resolved spectrum gives the electron intensity, I_E, as a function of the velocity, v_M, of He*(2^3S), the partial ionization cross section, $\sigma(E_c)$, can be determined by the following equations

$$\sigma(v_R) = c \frac{I_E(v_M)}{I_M(v_M)} \frac{v_M}{v_R} \tag{2}$$

and

$$v_R = \left[{v_M}^2 + \frac{3k_B T}{m} \right]^{1/2} \tag{3}$$

where c is a constant, v_R is the relative velocity averaged over the velocity of the target molecule, k_B is the Boltzmann constant, and T and m are the gas temperature and the mass of the target molecule. Finally, $\sigma(v_R)$ is converted to $\sigma(E_c)$ by the relation,

$$E_c = \mu {v_R}^2/2 \tag{4}$$

where μ is the reduced mass of the system.

The He I resonance line (584 Å, 21.22 eV) produced by a dc discharge in pure helium gas was utilized to measure the UPS. The electron spectra were obtained at an ejection angle of 90° with the same electron energy analyzer employed in the PIES measurements. The transmission of the electron energy analyzer was determined by comparing our UPS data with those by Gardner and Samson[30] and Kimura *et al.*[31]

III. Calculations

In order to discuss the interaction potential, interaction potential curves with the metastable atom approaching the cyclopropane and the amino group of the cyclopropylamine were calculated using the *ab initio* molecular orbital (MO) method in the scheme of the unrestricted Hartree−Fock (UHF). Since there are difficulties associated with calculations for excited states and a well-known resemblance between He*(2^3S) and Li(2^2S), a Li(2^2S) atom was used in the present study in place of He*(2^3S). As for this resemblance, it has been shown[32] that the shape of the velocity dependence of the total scattering cross section of He*(2^3S) by He, Ar, and Kr is very similar to that of Li(2^2S) and that the interaction potential well depths and the location of potential wells have also been found to be very similar for the interactions of various targets with He*(2^3S) and Li(2^2S) (see refs 2, 14, 33, and 34 and references cited therein). The structures of the neutral molecules were fixed at those taken from the literature.[35−37] All the calculations in this work were carried out using a quantum chemistry program.[38] A 4-31++G** basis set was used. For cyclopropane, the correlation energy correction was partially taken into account by using the second-order Møller-Plesset perturbation theory (MP2), and the full counterpoise method[39] was used to correct the basis set superposition errors.

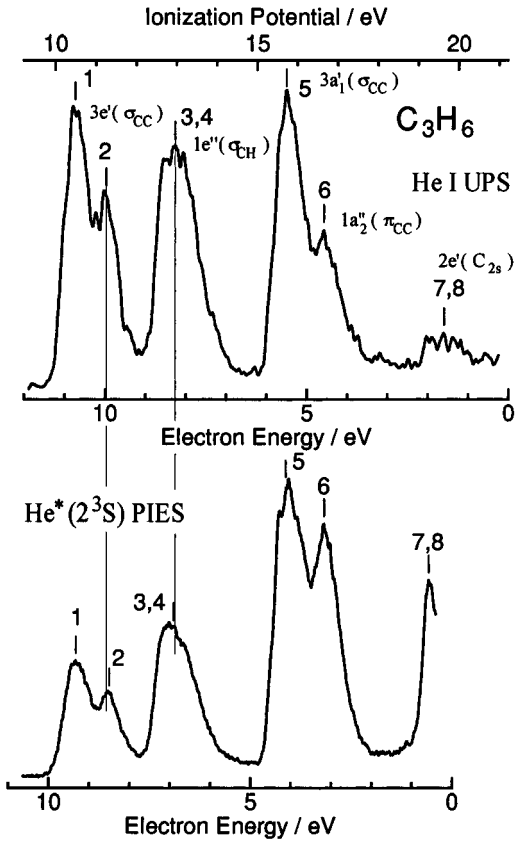

Figure 1. He I UPS and He*(2^3S) PIES of cyclopropane.

IV. Results

Figures 1−3 show the He I ultraviolet photoelectron spectra and Penning ionization electron spectra of cyclopropane, cyclopropylamine, and cyanocyclopropane, respectively. The electron energy scales for the PIES are shifted relative to those for the UPS by the difference in the excitation energies, 21.22 − 19.82 = 1.40 eV. The He I UPS are consistent with the earlier data.[31,40−42] Figures 4−6 show the CERPIES of cyclopropane, cyclopropylamine, and cyanocyclopropane, respectively. In each figure, the low collision energy spectra (*ca.* 100 meV) are shown by a solid curve, and the high collision energy spectra (*ca.* 250 meV) are shown by a dashed curve. The relative intensities of the two spectra are normalized in the figures using the data of the log σ *vs* log E_c plots cited below.

Table 1 lists the vertical ionization potentials (determined from the He I UPS) and the assignments of the observed bands. The peak energy shifts, ΔE, in PIES measured with respect to the nominal energy E_0 (E_0 = the difference between metastable excitation energy and target ionization potential) and calculated IP values using the 4-31G basis set are also shown in the table. Uncertainties of the peak positions were estimated to be about 10% of the band width using a Gaussian curve fitting.

Figures 7−9 show the log σ *vs* log E_c plots for cyclopropane, cyclopropylamine, and cyanocyclopropane, respectively. The calculated electron density maps and schematic representation of the molecular orbitals are also shown in the figures. In the

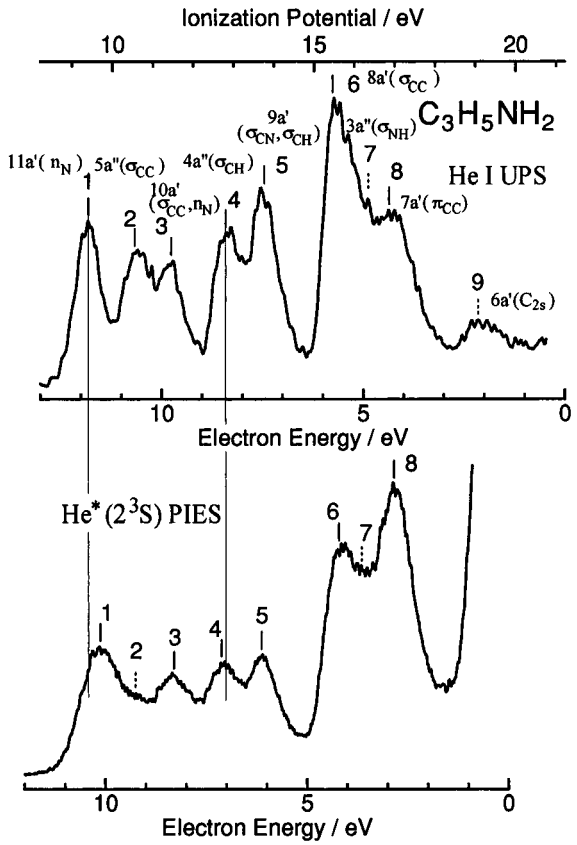

Figure 2. He I UPS and He*(2^3S) PIES of cyclopropylamine.

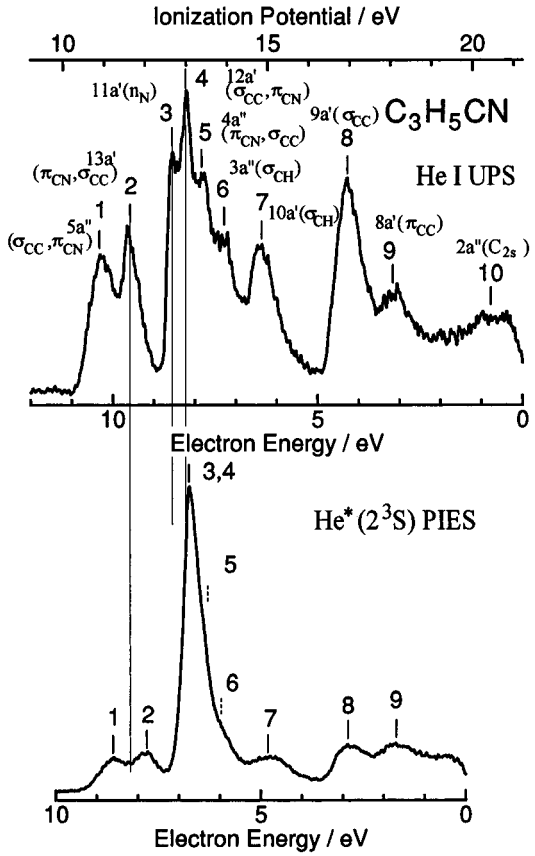

Figure 3. He I UPS and He*(2^3S) PIES of cyanocyclopropane.

electron density map, the C_3 ring plane or mirror symmetry plane was selected as the cutting plane as it is not a nodal plane. In the case of the 4a″ and 3a″ orbitals for cyclopropylamine as well as the a″ orbitals for cyanocyclopropane, the cutting plane

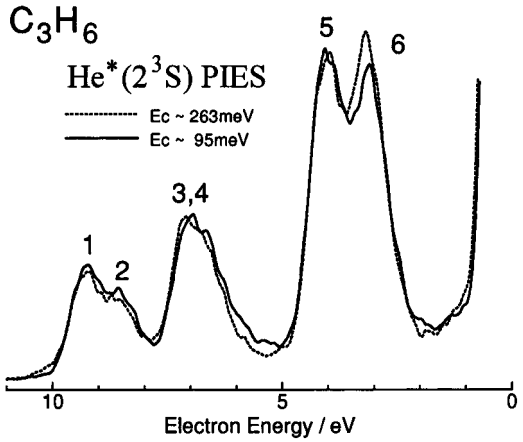

Figure 4. Collision energy resolved He*(2^3S) Penning ionization electron spectra of cyclopropane (dashed curve at $E_c = 263$ meV, solid curve 95 meV).

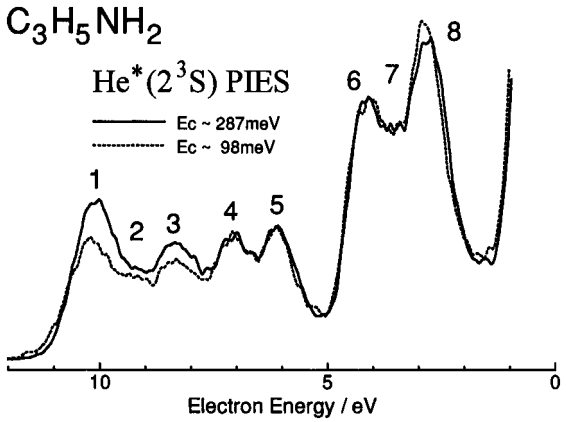

Figure 5. Collision energy resolved He*(2^3S) Penning ionization electron spectra of cyclopropylamine (dashed curve at $E_c = 287$ meV, solid curve 98 meV).

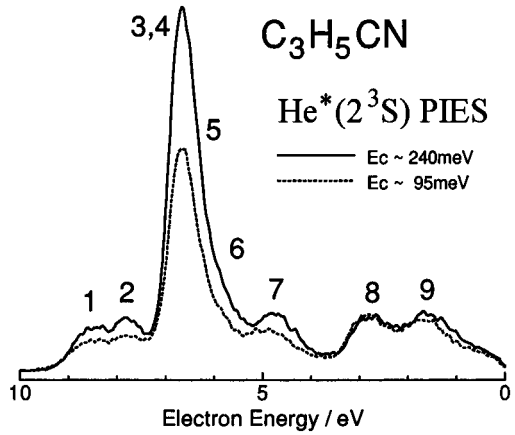

Figure 6. Collision energy resolved He*(2^3S) Penning ionization electron spectra of cyanocyclopropane (dashed curve at $E_c = 240$ meV, solid curve 95 meV).

is selected as the NH_2 plane or CN plane. The values of the slope m of the log σ *vs* log E_c plots estimated by a linear least-squares method are also listed in Table 1. Uncertainties associated with this measurement are *ca.* ±0.03.

Figure 10 shows the potential energy curves $V^*(R)$ obtained from the model potential calculations for cyclopropane. The distance R is measured from the center of the mass of a molecule. Figure 11 shows the isopotential energy contour maps for cyclopropane; the map for the molecular plane (a) and that for the out-of-plane (b) are separately shown. Contour lines are shown from 100 to 700 meV with an energy spacing of

TABLE 1: Band Assignments, Ionization Potential (IP), Peak Energy Shift (ΔE), and Obtained Parameters (m, s, d) for the Cyclopropanes (See Text)

molecule	band	IP (eV) obsd	IP (eV) calcd	orbital character	ΔE (meV)	m	s	d (au^{-1})
C_3H_6	1	10.49	11.33	$3e'(\sigma_{CC})$	-25 ± 40	-0.09		4.27
	2	11.26	11.33	$3e'(\sigma_{CC})$	-65 ± 45	-0.08		4.17
	3, 4	12.96	13.83	$1e''(\sigma_{CH})$	40 ± 80	0.01		3.43
	5	15.73	16.87	$3a_1'(\sigma_{CC})$	25 ± 45	-0.01		3.57
	6	16.65	18.22	$1a_2''(\pi_{CC})$	10 ± 70	0.12		2.82
	7, 8	(19.62)	22.13	$2e'(C_{2s})$				
$C_3H_5NH_2$	1	9.40	10.12	$11a'(n_N)$	-290 ± 60	-0.26	7.69	
	2	10.55	10.97	$5a''(\sigma_{CC})$		-0.13	15.38	
	3	11.45	11.93	$10a'(\sigma_{CC},n_N)$	-65 ± 75	-0.18	11.11	
	4	12.80	13.84	$4a''(\sigma_{CH})$	110 ± 50	-0.05		3.69
	5	13.76	14.92	$9a'(\sigma_{CN},\sigma_{CH})$	70 ± 70	-0.04		3.61
	6	15.47	16.77	$8a'(\sigma_{CC})$	-140 ± 80	0.02		3.20
	7	(16.3)	17.50	$3a''(\sigma_{NH})$		-0.02		3.46
	8	16.86	18.56	$7a'(\pi_{CC})$	-120 ± 90	0.03		3.13
	9	(19.3)	21.55	$6a'(C_{2s})$				
C_3H_5CN	1	10.88	11.22	$5a''(\sigma_{CC},\pi_{CN})$	-330 ± 50	-0.38	5.26	
	2	11.63	11.95	$13a'(\pi_{CN},\sigma_{CC})$	-400 ± 50	-0.41	4.88	
	3	12.66	14.74	$11a'(n_N)$	-400 ± 20	-0.52	3.85	
	4	12.99	13.47	$12a'(\sigma_{CC},\pi_{CN})$				
	5	13.38	14.24	$4a''(\pi_{CN},\sigma_{CC})$				
	6	13.93	14.93	$3a''(\sigma_{CH})$	80 ± 40	-0.45	4.44	
	7	14.84	16.27	$10a'(\sigma_{CH})$	-150 ± 75	-0.38	5.26	
	8	16.93	18.64	$9a'(\sigma_{CC})$	-10 ± 50	0.02		3.44
	9	18.06	19.97	$8a'(\pi_{CC})$	-70 ± 80	-0.16	12.5	
	10	(20.45)	23.24	$2a''(C_{2s})$				

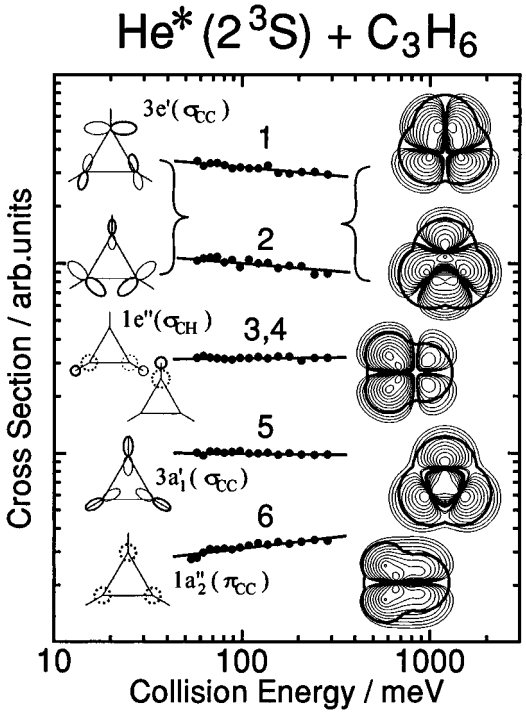

Figure 7. Collision energy dependence of partial ionization cross sections for cyclopropane that collided with He*(2^3S).

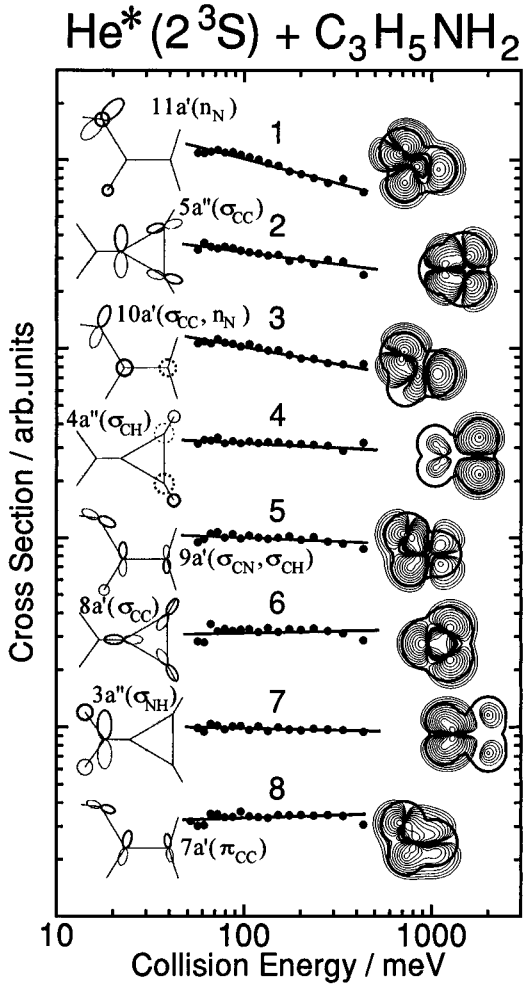

Figure 8. Collision energy dependence of partial ionization cross sections for cyclopropylamine that collided with He*(2^3S).

100 meV. Figure 12 shows the potential energy curves $V^*(R)$ obtained from the model potential calculations for cyclopropylamine. The distance R is measured from the nitrogen atom. The He* (Li) atom is located in the direction bisecting the angle of C−N−P, where P is the midpoint of the two hydrogen atoms in the amino group.

V. Discussion

A. A Simple Model for CEDPICS. Penning ionization electron spectroscopy is similar to ultraviolet photoelectron spectroscopy since the kinetic energy of electrons ejected upon ionization is analyzed. The relative band intensities of PIES and UPS are, however, very different, reflecting the difference in their ionization mechanism.[43] In the Penning ionization

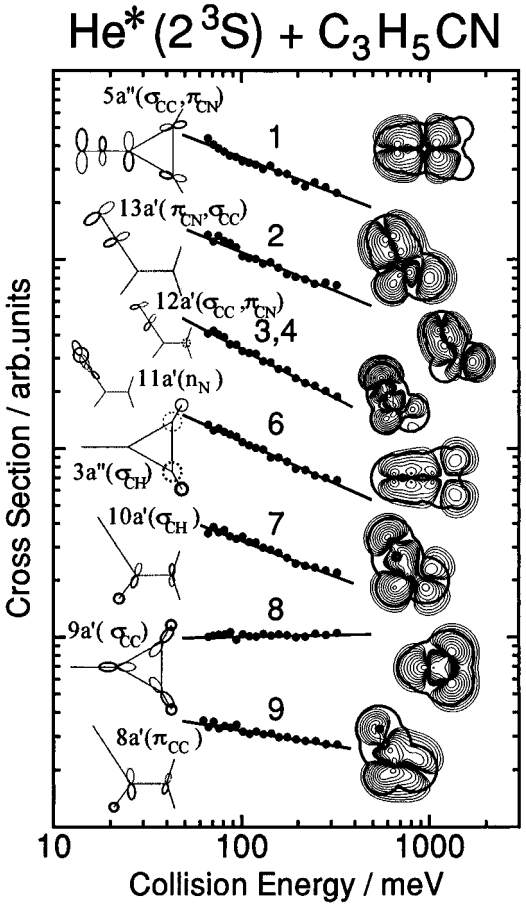

Figure 9. Collision energy dependence of partial ionization cross sections for cyanocyclopropane that collided with He*(2^3S).

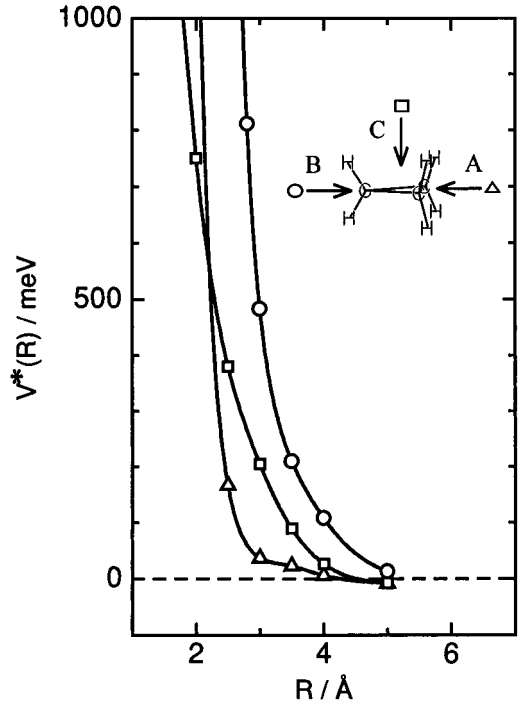

Figure 10. Model potential curves $V^*(R)$ for cyclopropane−He*: (△, direction A) the potential energy curve for in-plane access to the center of the CC bond; (○, direction B) the potential energy curve for in-plane access to the carbon atom; (□, direction C) the potential energy curve for out-of-plane access to the center of mass of the molecule. The distance R is measured from the center of the mass of the molecule.

process, an electron in a molecular orbital of the target molecule (M) is transferred to the inner-shell orbital of a metastable atom

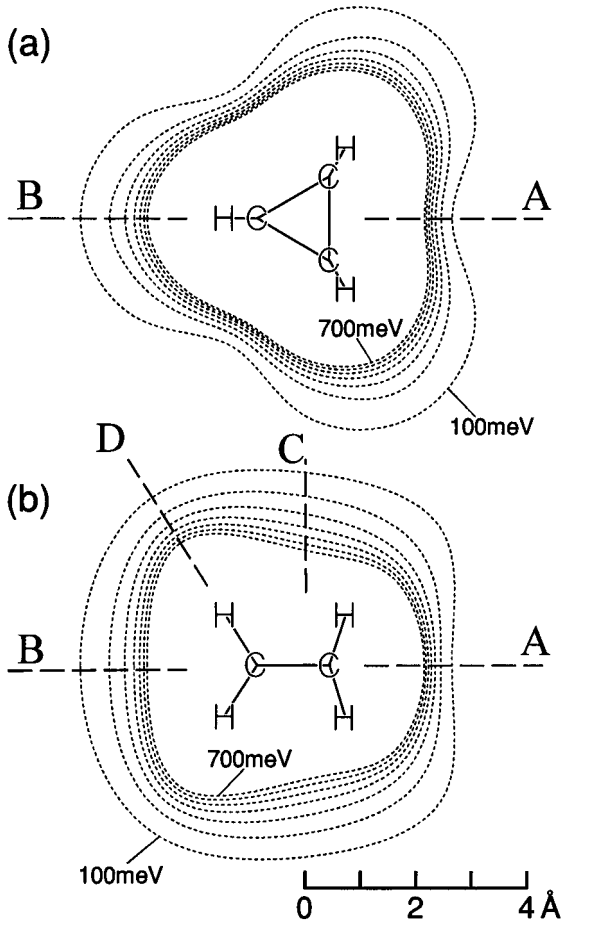

Figure 11. Potential energy contour maps for cyclopropane: (a) contours for the molecular plane; (b) contours for the out-of-plane. Contours are shown from 100 to 700 meV with an energy spacing of 100 meV. Direction A corresponds to in-plane access to the center of the CC bond, direction B to in-plane access to the carbon atom, direction C to out-of-plane access to the center of the mass of the molecule, and direction D to direct access to the hydrogen atom. The order of the spacing of the contour lines in this energy region is A < D < B < C.

(A*), and the excited electron of A* is ejected.[44] The probability of the electron transfer from M to A* largely depends on the spatial overlap between the orbitals of M and A*. The relative band intensity of PIES, therefore, reflects the electron distribution of individual molecular orbitals exposed outside the molecular surface.[43]

For the isotropic target system, a simple model for the collision energy dependence of $\sigma(E)$ (band intensity) has been established.[2,4,9] This model is applicable to qualitatively understanding CEDPICS and CERPIES of anisotropic molecules.

If the long range attractive part of the interaction potential $V^*(R)$ plays a dominant role and its function form is the type of $V^*(R) \propto R^{-s}$, the negative slope m of the log $\sigma(E_c)$ *vs* log E_c plots is approximately described as[2,4,9]

$$m = -2/s \tag{5}$$

The s value represents the steepness of the attractive part of the interaction potential curve. In other words, the large absolute value of negative m indicates a long range attractivity. If the metastable atom is a rare gas atom, the attractive interaction in the outgoing channel of the ionization process is very weak and the potential well depth, ϵ^*, of the interaction potential V^* can be roughly estimated by the peak shift.[45]

On the other hand, if the repulsive part of the interaction potential governs the energy dependence, the slope m of the

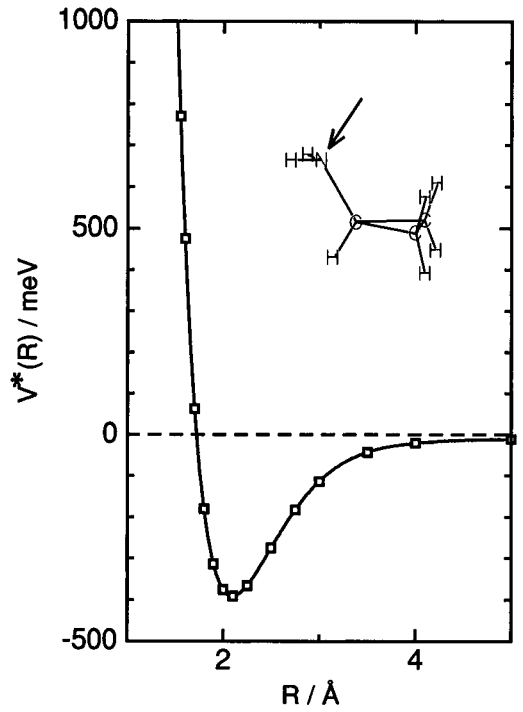

Figure 12. Model potential curves $V^*(R)$ for cyclopropylamine−He*. The distance R is measured from the nitrogen atom. The He* (Li) atom is located in the direction bisecting the angle of C−N−P, where P is the midpoint of the two hydrogen atoms in the amino group.

log $\sigma(E_c)$ *vs* log E_c plots can be related approximately to the parameter d (effective steepness or hardness of the repulsive potential wall; $V^*(R) \propto \exp(-dR)$)[4,14] by

$$m = 2\{2I(\mathrm{M})\}^{1/2}/d - 1/2 \qquad (6)$$

where I(M) is the lowest ionization potential.

Since a molecular orbital is more or less localized on a special part of the molecule and the Penning ionization occurs in a high electron density area, the slope parameter of CEDPICS reflects the information about the anisotropic interaction potential.

B. Cyclopropane. Figure 1 shows the UPS and PIES of cyclopropane. Our assignments of this compound are the same as those reported by Basch *et al.*[40] Bands 1 and 2, which are split by the Jahn-Teller effect, are assigned to the $\sigma_{CC}(3e')$ orbitals. Since incoming interaction potentials corresponding to these bands are the same, the slope parameter, m, of these bands are almost the same, −0.09 and −0.08, and the peak energy shifts, ΔE, are −25 and −65 meV, respectively. These values suggest that there exists a shallow potential well and that the repulsive potential wall is very hard; the decay parameters d are 4.27 and 4.17, respectively, as shown in Table 1.

Bands 3 and 4 are assigned to the $\sigma_{CH}(1e'')$ orbital, which is mainly distributed around the hydrogen atoms. The positive peak energy shift of $\Delta E = 40$ meV and small slope parameter of $m = 0.01$ show the existence of a repulsive potential wall around the hydrogen atoms as in the case of CH_3CN[23] and C_6H_6.[16] This is also supported by the fact that the peak position of this band in the hot spectrum is shifted to the higher electron energies compared with cold one in the CERPIES (see Figure 4).

Band 5 is assigned to the $\sigma_{CC}(3a_1')$ orbital, which is distributed near the hydrogen atoms in the C_3 carbon ring plane. Since this orbital extends near the hydrogen atom, the obtained repulsive decay parameter ($d = 3.57$) is near the value for that of bands 3 and 4 ($d = 3.43$).

Band 6 is assigned to the $\pi_{CC}(1a_2'')$ orbital, which is mainly distributed vertically to the carbon ring plane. The slope parameter, m, is the largest in this compound ($m = 0.12$), and this means that the repulsive interaction potential with the He*-(2^3S) atom is relatively soft. This is supported by the peak energy shift in the CERPIES (see Figure 7) as in the case of bands 3 and 4. This behavior is compared to that of benzene.[16] In benzene, a clear attractive interaction has been observed in the π orbital region. This difference is possibly due to the difference in the donative nature of the π electrons or due to the existence of hydrogen atoms.

Judging from the enhancement in the PIES, bands 7 and 8 seem to be assigned to the $C_{2s}(2e')$ bands. For hydrocarbons which contain multiple carbon atoms, the C_{2s} bands show enhancement in PIES due to the formation of an excimer-like state partly involving a C_{2s} type hole in the target molecule which facilitates selective intramolecular Auger-like transitions from orbitals having the C_{2s} character.[15]

These findings lead to the propensity that the order of the hardness parameter of the repulsive interaction potential is $\pi_{CC} < \sigma_{CH} < \sigma_{CC}$. This is consistent with the model potential curves in Figure 10 and potential contour maps in Figure 11. In Figure 11, the contour lines are closely spaced in the A direction, and this means a steep repulsive wall indicating a hard repulsive potential. In the B and D directions, the spacing of the contour lines is moderate. In the C direction, the spacing is rather wide; this means a more flattened slope indicating a soft repulsive interaction potential.

C. Cyclopropylamine. The UPS of cyclopropylamine ($C_3H_5NH_2$) has been previously investigated by Kimura *et al.*,[31] and our assignments are essentially the same as their assignments. Band 7, which was overlooked in a previous study,[31] can be assigned to the $\sigma_{NH}(3a'')$ band. Although this band is not clear in the UPS and PIES, the spectral region between band 6 and band 8 behaves differently from the neighboring bands in Figure 5. The existence of band 7 is confirmed by the present CERPIES.

Band 1 is assigned to $n_N(11a')$ orbital, which is distributed around the nitrogen atom. This band shows a strong negative peak energy shift ($\Delta E = -290$ meV) and large negative inclination of the slope parameter ($m = -0.26$). This fact shows that the nitrogen atom strongly attracts He*(2^3S) atoms. As shown in Figure 12, this tendency is clearly supported by the calculated interaction potential. As in the case of CH_3CN and CH_3NC,[23] these also predict the existence of stable $C_3H_5NH_2$-Li radicals.

Though band 2 is assigned to the $\sigma_{CC}(5a'')$ orbital, it is largely overlapped by band 1. Hence, its slope parameter and the value of the peak shift must be affected by band 1. It is certain that the attractive interaction around the σ_{CC} orbital is weaker than that of the n_N region.

Band 3 is assigned to the σ_{CC}, $n_N(10a')$ orbital. Since this band has both σ_{CC} and n_N character, behavior of the slope parameter, m, and the peak energy shift, ΔE, are moderate reflecting the character of n_N and σ_{CC} as described below.

As for the characteristics of the σ_{CC} band, behavior of band 6 is important. This band is assigned to the $\sigma_{CC}(8a')$ orbital, which is mainly distributed around the carbon atoms in its ring plane. The slope parameter, m, of this band is 0.02, and this value is quite close to that of the corresponding $\sigma_{CC}(3a'_1)$ band of cyclopropane ($m = -0.01$). This means that behavior of this band is not significantly affected by the existence of the attractive substituent group.

In this relation, the behavior of band 8, which is assigned to the $\pi_{CC}(7a')$ orbital, is remarkable. The slope parameter, m, of

this band is 0.03, though that of cyclopropane is 0.12. This means that He*(2^3S) metastable atoms, which react with π_{CC} orbital, are affected by attractive interaction around the substituent NH_2 group.

Though band 7 is weak in the He I UPS and He*(2^3S) PIES, it is certain that there exists a band with a negative collision energy dependence between bands 6 and 8 which shows a positive collision energy dependence (see Figure 5). Since band 7 shows a negative collision energy dependence, it is reasonable that this band is assigned to the σ_{NH} band.

Bands 4 and 5 are assigned to the σ_{CH}(4a″) and σ_{CN},σ_{CH}-(9a′) bands, and the slope parameters are −0.05 and −0.04, respectively. Compared with the corresponding values of bands 3 and 4 in cyclopropane ($m = 0.01$), these values show a larger negative collision energy dependence. This means that the trajectory of He* which reacts with these orbitals is affected by the attractive interaction around the NH_2 group as in the case of the π_{CC} orbital.

D. Cyanocyclopropane. The UPS of cyanocyclopropane (C_3H_5CN) has been investigated by Turner *et al.*[41] and Gochel-Dupuis *et al.*[42] Gochel-Dupuis *et al.* have proposed its assignment using OVGF and ADC(3) calculations. Our assignments based on the present PIES measurement agree with their assignments except for band 3 and band 4. Though Gochel-Dupuis *et al.* have assigned band 3 to the 12a′ orbital and band 4 to the 11a′ orbital considering the configuration interaction, we assigned these two bands by means of collision energy resolved PIES; the assignments for bands 3 and 4 are n_N(11a′) and σ_{CC},π_{CN}(12a′), respectively. The reasons for these assignments are as follows.

(1) Band 3 shows remarkable enhancement in PIES. It is known that the n_N band shows large enhancement in PIES.[23,26,46]

(2) Although bands 3 and 4 are overlapped in PIES, the component of band 3 is dominant. Thus the slope parameter, *m*, for band 3 is estimated to be −0.52, and its negative peak shift is $\Delta E = -400$ meV. These large negative values strongly suggest that this band is assigned to the n_N orbital, since it is known that the n_N band shows a large negative slope parameter, *m*,[23,26] and shows a large negative peak shift,[23,26,46] reflecting its strong attractive interaction potential around the nitrogen lone pair.

(3) Calculated IP values from the *ab initio* MO energies for the n_N orbitals in acetonitrile, propionitrile, and *n*-butyronitrile are 0.86−1.81 eV smaller than the observed IP values.[46] If this propensity is transferred to cyanocyclopropane, the IP value for the n_N orbital of cyanocyclopropane is estimated to be 12.93−13.88 eV, which corresponds to the observed IP value for band 3 (12.66 eV).

Thus bands 3 and 4 are assigned to the n_N(11a′) orbital and σ_{CC},π_{CN}(12a′) orbital, respectively. As for the attractive interactions around the nitrogen lone pair for the n_N band of cyclopropylamine and cyanocyclopropane, negative peak energy shifts are $\Delta E = -290$ and −400 meV, respectively, and the slope parameters are $m = -0.26$ and −0.52, respectively. Thus the order of the attractive interaction around the nitrogen atom is NH_2 < CN. On the basis of the calculated results, attractive interactions around the nitrogen lone pair for n_N bands are estimated to be the same (*ca.* −400 meV) for the NH_2 and CN[23,26] groups. Hence, the order of the observed effective attractive interaction for the NH_2 and CN groups is thought to reflect the stereochemical environment around the lone pair.

Band 1 and band 2 are assigned to the σ_{CC},π_{CN}(5a″) and π_{CN},σ_{CC}(13a′) orbitals, respectively. These bands also show large negative slopes ($m = -0.38$ and −0.41, respectively) and large negative peak shifts ($\Delta E = -330$ and −400 meV, respectively), reflecting the attractive interaction around the CN group.

Bands 5 and 6 are assigned to the π_{CN},σ_{CH}(4a″), σ_{CH}(3a″) orbitals, respectively. Since they are strongly overlapped with band 3 and band 4, it is difficult to obtain information on interaction potentials.

Band 7 is assigned to the σ_{CH}(10a′) orbital. Since this orbital extends its electron density both around the hydrogen atoms and around the n_N region, the slope parameter reflects the characteristics that the negative inclination ($m = -0.38$) is smaller than that of the pure n_N(11a′) orbital ($m = -0.52$).

Band 8 is assigned to the σ_{CC}(9a′) orbital, which is distributed around the carbon atoms in the carbon ring plane. This band corresponds to band 5 of the cyclopropane and to band 6 of the cyclopropylamine, and the slope parameters of these bands are almost the same ($m = 0.02$, −0.01, and 0.02, respectively). As discussed in section C, this suggests that the substituent groups of these compounds do not effectively deflect the incoming trajectory from the in-plane direction.

On the other hand, band 9, which is assigned to the π_{CC}(8a′) orbital, has a larger negative inclination ($m = -0.16$) compared with those of the corresponding bands for cyclopropane (band 6, $m = 0.12$) and cyclopropylamine (band 8, $m = 0.03$). Since the negative peak shifts of these bands are not large ($\Delta E = -70$, 10, −120 meV, respectively) compared with the measured collision energy range, a systematic change in the slope parameter seems to be an effect of the attractive interaction on the He* trajectory. This trend is in good agreement with the relative magnitude of the slope parameter, *m*, of the n_N orbitals.

VI. Conclusions

(1) In cyclopropane, interactions around the C_3 carbon ring and the hydrogen atom with He*(2^3S) are repulsive. The relative hardness of the repulsive potentials (as shown in *d* parameter in Table 1) was found to be as follows: C_3 ring (out-of-plane direction) < hydrogen atoms < C_3 ring (in-plane direction).

(2) The interaction potentials around the nitrogen atom of the NH_2 group and CN group in the cyclopropanes are strongly attractive. The magnitude of this attractive interaction is NH_2 < CN.

(3) Model potential calculations support the experimental result of (1) and the existence of the potential well around the NH_2 and CN[23,26] groups. These also predict the existence of stable $C_3H_5NH_2Li$ and C_3H_5CNLi radicals.

(4) The attractive interaction mentioned in (2) seems to affect the trajectory of the He*(2^3S)s which mainly react with the π_{CC} orbitals from the out-of-plane direction. On the contrary, this effect is hardly seen in the reaction with σ_{CC} orbitals, which is distributed in the C_3 carbon ring plane. This is probably because the trajectories of He*, which react with σ_{CC} orbitals in in-plane directions, are far from the attractive substituent group.

(5) The assignments of the UPS of cyclopropylamine and cyanocyclopropane were also reinvestigated using the present collision energy resolved PIES.

Acknowledgment. This work has been supported by a Grant-in-Aid for Scientific Research from the Japanese Ministry of Education, Science, and Culture.

References and Notes

(1) Penning, F. M. *Naturwissenschaften* **1927**, *15*, 818.
(2) Niehaus, A. *Adv. Chem. Phys.* **1981**, *45*, 399.

(3) Yencha, A. J. *Electron Spectroscopy: Theory, Technique, and Applications*; Brundle, C. R., Baker, A. D., Eds.; Academic: New York, 1984; Vol. 5.
(4) Illenberger, E.; Niehaus, A. *Z. Phys. B* **1975**, *20*, 33.
(5) Parr, T. P.; Parr, D. M.; Martin, R. M. *J. Chem. Phys.* **1982**, *76*, 316.
(6) Pesnelle, A.; Watel, G.; Manus, C. *J. Chem. Phys.* **1975**, *62*, 3590.
(7) Woodard, M. R.; Sharp, R. C.; Seely, M.; Muschlitz, E. E., Jr. *J. Chem. Phys.* **1978**, *69*, 2978.
(8) Appolloni, L.; Brunetti, B.; Hermanussen, J.; Vecchiocattivi, F.; Volpi, G. G. *J. Chem. Phys.* **1987**, *87*, 3804.
(9) Allison, W.; Muschlitz, E. E., Jr. *J. Electron Spectrosc. Relat. Phenom.* **1981**, *23*, 339.
(10) Riola, J. P.; Howard, J. S.; Rundel, R. D.; Stebbings, R. F. *J. Phys. B* **1974**, *7*, 376.
(11) Lindinger, W.; Schmeltekopf, A. L.; Fehsenfeld, F. C. *J. Chem. Phys.* **1974**, *61*, 2890.
(12) Čermák, V. *J. Chem. Phys.* **1966**, *44*, 3781.
(13) Mitsuke, K.; Takami, T.; Ohno, K. *J. Chem. Phys.* **1989**, *91*, 1618.
(14) Ohno, K.; Takami, T.; Mitsuke, K.; Ishida, T. *J. Chem. Phys.* **1991**, *94*, 2675.
(15) Takami, T.; Mitsuke, K.; Ohno, K. *J. Chem. Phys.* **1991**, *95*, 918.
(16) Takami, T.; Ohno, K. *J. Chem. Phys.* **1992**, *96*, 6523.
(17) Dunlavy, D. C.; Martin, D. W.; Siska, P. E. *J. Chem. Phys.* **1990**, *93*, 5347.
(18) Longley, E. J.; Dunlavy, D. C.; Falcetta, M. F.; Bevsek, H. M.; Siska, P. E. *J. Phys. Chem.* **1993**, *97*, 2097.
(19) Siska, P. E. *Rev. Mod. Phys.* **1993**, *65*, 337.
(20) Pasinszki, T.; Yamakado, H.; Ohno, K. *J. Phys. Chem.* **1993**, *97*, 12718.
(21) Ohno, K.; Kishimoto, N.; Yamakado, H. *J. Phys. Chem.* **1995**, *99*, 9687.
(22) Ohno, K.; Okamura, K.; Yamakado, H.; Hoshino, S.; Takami, T.; Yamauchi, M. *J. Phys. Chem.* **1995**, *99*, 14247.
(23) Pasinszki, T.; Yamakado, H.; Ohno, K. *J. Phys. Chem.* **1995**, *99*, 14678.
(24) Yamakado, H.; Yamauchi, M.; Hoshino, S.; Ohno, K. *J. Phys. Chem.* **1995**, *99*, 17093.
(25) Kishimoto, N.; Yamakado, H.; Ohno, K. *J. Phys. Chem.* **1996**, *100*, 8204.
(26) Kishimoto, N.; Aizawa, J.; Yamakado, H.; Ohno, K. *J. Phys. Chem.*, submitted for publication.
(27) Yamauchi, M.; Yamakado, H.; Ohno, K. *J. Phys. Chem.*, submitted for publication.
(28) Kudo, H.; Hashimoto, M.; Yokoyama, K.; Wu, C. H.; Dorigo A. E.; Bickelhaupt, F. M.; Schleyer, P. v. R. *J. Phys. Chem.* **1995**, *99*, 6477.
(29) Mitsuke, K.; Kusafuka, K.; Ohno, K. *J. Phys. Chem.* **1989**, *93*, 3062.
(30) Gardner, J. L.; Samson, J. A. R. *J. Electron Spectrosc. Relat. Phenom.* **1976**, *8*, 469.
(31) Kimura, K.; Katsumata, S.; Achiba, Y.; Yamazaki, T.; Iwata, S. *Handbook of HeI Photoelectron Spectra of Fundamental Organic Molecules*; Japan Scientific: Tokyo, 1981.
(32) Rothe, E. W.; Neynaber, R. H.; Trujillo, S. M. *J. Chem. Phys.* **1965**, *42*, 3310.
(33) Hotop, H. *Radiat. Res.* **1974**, *59*, 379.
(34) Haberland, H.; Lee, Y. T.; Siska, P. E. *Adv. Chem. Phys.* **1981**, *45*, 487.
(35) Bastiansen, O.; Fritsch, F. N.; Hedberg, K. *Acta Crystallogr.* **1964**, *17*, 538.
(36) Hendricksen, D. K.; Harmony, M. D. *J. Chem. Phys.* **1969**, *51*, 700.
(37) Harmony, M. D.; Nandi, R. N.; Tietz, J. V.; Choe, J.-I., Getty, S. J.; Staley, S. W. *J. Am. Chem. Soc.* **1983**, *105*, 3947.
(38) Frisch, M. J.; Trucks, G. W.; Head-Gordon, M.; Gill, P. M.; Wong, M. W.; Foresman, J. B.; Johnson, B. G.; Schlegel, H. B.; Robb, M. A.; Replogle, E. S.; Gomperts, R.; Andres, J. L.; Raghavachari, K.; Binkley, J. S.; Gonzalez, C.; Martin, R. L.; Fox, D. J.; Defrees, D. J.; Baker, J.; Stewart, J. J. P.; Pople, J. A. *Gaussian 92*; Gaussian Inc.: Pittsburgh, PA, 1992.
(39) Boys, S. F.; Bernardi, F. *Mol. Phys.* **1970**, *19*, 553.
(40) Basch, H.; Robin, M. B.; Kuebler, N. A.; Baker, C.; Turner, D. W. *J. Chem. Phys.* **1969**, *51*, 52.
(41) Turner, D. W.; Baker, C.; Baker, A. D.; Brundle, C. R. *Molecular Photoelectron Spectroscopy*; Wiley-Interscience: London, 1970.
(42) Gochel-Dupuis, M.; Ohno, M.; von Niessen, W.; Heinesch, J.; Delwiche, J. *Chem. Phys. Lett.* **1995**, *232*, 301.
(43) (a) Ohno, K.; Mutoh, H.; Harada, Y. *J. Am. Chem. Soc.* **1983**, *105*, 4555. (b) Ohno, K.; Harada, Y. *Theoretical Models of Chemical Bonding*, Part 3; Maksić, Z. B., Ed.; Springer-Verlag: Berlin, 1991; pp 199−234.
(44) Hotop, H.; Niehaus, A. *Z. Phys.* **1969**, *228*, 68.
(45) Niehaus, A. *Ber. Bunsen-Ges. Phys. Chem.* **1973**, *77*, 632.
(46) Ohno, K.; Matsumoto, S.; Imai, K.; Harada, Y. *J. Phys. Chem.* **1984**, *88*, 206.